Local vibrational modes in crystal lattices with a simply connected region of the quasi-continuous phonon spectrum

Cite as: Low Temp. Phys. **32**, 256 (2006); https://doi.org/10.1063/1.2178484
Published Online: 03 April 2006

A. V. Kotlyar, and S. B. Feodosyev

LATTICE DYNAMICS

Local vibrational modes in crystal lattices with a simply connected region of the quasi-continuous phonon spectrum

A. V. Kotlyar[a] and S. B. Feodosyev

B. Verkin Institute for Low Temperature Physics and Engineering, National Academy of Sciences of Ukraine, pr. Lenina 47, Kharkov 61103, Ukraine

(Submitted September 19, 2005; revised October 7, 2005)
Fiz. Nizk. Temp. **32**, 343–359 (March 2006)

It is shown that the use of the mode classification adopted in the Jacobi matrix method and which is the most natural one for describing localized states leads to extremely rapid convergence of the Green functions for frequencies lying outside the quasi-continuum band of the crystal. This has made it possible to obtain rather general analytical expressions for the conditions of formation and the characteristics of local modes due to the presence of light impurity atoms in crystal lattices having a simply connected region of the quasi-continuous phonon spectrum. The accuracy with which the frequencies and intensities of the local modes are determined using these expressions is illustrated for examples of light substitutional impurities (isotopic and weakly coupled) and close-packed structures (fcc and hcp) and also isolated pairs of isotopic impurities in an fcc crystal lattice. In particular, the results permit simple and extremely accurate evaluation of the parameters of the host lattice and defect from the known values of the local frequencies. © *2006 American Institute of Physics*. [DOI: 10.1063/1.2178484]

INTRODUCTION

Discrete levels arising outside the quasi-continuum band of the phonon spectrum of the ideal lattice of a crystal when light or strongly coupled impurities are introduced in it have been known and studied both theoretically and experimentally for around sixty years. The amplitudes of the corresponding vibrations, which are called local modes, fall off rapidly with distance from the defect, and at distances from the impurity atom much greater than the characteristic radius of the interatomic interaction in the lattice their decay can be considered exponential. The now classic results in the papers by I. M. Lifshits and his school,[1–6] in which the theory of regular degenerate perturbations was developed and used to obtain closed expressions for the changes of the phonon spectrum of a crystal due to local defects, including expressions for the frequencies of local vibrational modes, can be found in practically all textbooks on the dynamics of the crystal lattice, e.g., Refs. 7–11.

Since that time, experimental techniques have been developed for investigating local modes, the most efficient and most often used being neutron diffraction, spin-lattice relaxation, and optical and point-contact spectroscopy, which have made it possible to observe such oscillations in a number of solid solutions (see, e.g., Refs. 10, 12, and 13). The transformation of local levels in the quasiparticle spectra (phonon, electron, etc.) into impurity bands in crystals with a finite concentration of impurity atoms has been studied theoretically.[14–17] With the development of methods of nonlinear dynamics have come papers devoted to the influence of lattice anharmonicities on the local modes (see, e.g., Ref. 18).

However, to this day there is a lack of adequate expressions, even in the harmonic approximation, for describing the formation and basic characteristics of local modes (such as the local frequency and the amplitude of the impurity atom itself at that frequency and also the damping of the amplitude of the local mode with distance from the impurity) in the model of a crystal lattice with an isolated defect.

In this paper we obtain suitable analytical expressions for the case of light (isotopic and weakly coupled) substitutional impurities in crystals having a simply connected quasi-continuous spectrum. The results are analyzed in detail for close-packed lattices, when in the description of the interatomic interaction one can restrict consideration to the central interaction of nearest neighbors. The formulas describe the characteristics of the local modes to high accuracy over a wide frequency range and can be used to determine the parameters of the host lattice and of the impurity from experimentally measured local frequencies.

I. APPROXIMATING EXPRESSIONS FOR THE CHARACTERISTICS OF LOCAL MODES

The equation of the harmonic vibrations of a system of interacting oscillators (not necessarily having crystalline order) can be written in operator form as an eigenvalue problem for a certain operator $\hat{L}$ (see, e.g., Refs. 7, 8, and 11):

$$(\hat{L} - \lambda \hat{I})\vec{\psi} = 0. \tag{1}$$

In Eq. (1) the vector field $\psi(\mathbf{r})$ is a renormalized field of atomic displacements $\mathbf{u}(\mathbf{r})$:

$$u_i(\mathbf{r},t) \equiv \frac{\psi_i(\mathbf{r})}{\sqrt{m(\mathbf{r})}} e^{i\omega t} \tag{2}$$

and is treated as a certain vector space that we shall denote as H, i.e., $\vec{\psi}_p \equiv (\mathbf{r}_p; \psi(\mathbf{r}_p)) \in H$. The dimension of this space in

the general case is equal to the product of the number of atoms N in the system and the number of degrees of freedom q of each atom.[1)] In Eq. (2) $u_i(\mathbf{r},t)$ is the ith component of the displacement vector of an atom with radius vector $\mathbf{r}$ at time t; $m(\mathbf{r})$ is the mass of that atom, and $\lambda=\omega^2$ is the square of the eigenfrequency, which is the eigenvalue of the operator $\hat{L}$,

$$L_{ik}^{\mathbf{r},\mathbf{r}'}=\frac{\Phi_{ik}(\mathbf{r},\mathbf{r}')}{\sqrt{m(\mathbf{r})m(\mathbf{r}')}}, \tag{3}$$

acting in the space H [$\Phi_{ik}(\mathbf{r},\mathbf{r}')$ is the matrix of force constants].

The vibrations of a crystal lattice containing an isolated point defect are described by the operator $\hat{L}=\hat{L}_0+\hat{\Lambda}$, where the operator $\hat{L}_0$ describes the vibrations of the unperturbed (ideal) lattice and the operator $\hat{\Lambda}$ is the perturbation introduced by the defect. The discrete local levels satisfy the Lifshits equation, which can be written in operator form as (see, e.g., Ref. 11)

$$\det\| \hat{I}-\hat{G}_0(\lambda)\hat{\Lambda}\|=0. \tag{4}$$

Here $\hat{I}$ is the unit operator, and $\hat{G}_0(\lambda)$ is the Green operator of the unperturbed lattice, which for an arbitrary operator $\hat{L}$ is defined as

$$\hat{G}(\lambda)\equiv(\lambda\hat{I}-\hat{L})^{-1}. \tag{5}$$

If the operator matrix $\hat{\Lambda}$ has a finite rank, the perturbation is called degenerate, in which case Eq. (4) can be solved. The rank of a matrix depends not only on the form of the perturbation operator but also on the choice of basis. The conventional representation of lattice modes as a superposition of plane waves unjustifiably narrows the domain of applicability of the Lifshits equation, since many perturbation operators describing the influence of a point defect on the vibrational modes of a crystal lattice have a finite rank in the coordinate representation but an infinite rank in $\mathbf{k}$ space. The solution of this equation is also made difficult by the infinite degeneracy of the eigenmodes. To avoid these difficulties the J matrix method is used,[20,21] since the mode classification used in that method is most convenient for describing the bound states, and the spectra of the operators considered in that method are simple. The J matrix method is set forth in detail in Refs. 20–23 and in the Appendix to Ref. 24, where it is used specifically to describe local modes. Therefore, in this paper we shall give a minimal introduction to the J matrix method to permit the reader to understand the terminology used and the results obtained.

A. Evaluation of the Green function by the *J* matrix method

The J matrix method is based on dividing up the mode space H into a sum of subspaces, each of which is specified by a choice of a certain generating vector $\vec{h}_0\in H$, corresponding to a certain displacement of some selected atom or group of atoms. In each such subspace the Green function $G(\lambda)$—the matrix element of the Green operator $G(\lambda)\equiv G_{00}(\lambda)\equiv(\vec{h}_0,\hat{G}(\lambda)\vec{h}_0)$—is represented as a continued or chain fraction, which contracts to the form[22,23]

$$G(\lambda)=\lim_{n\to\infty}G_{(n)}(\lambda);$$

$$G_{(n)}(\lambda)=\frac{Q_n(\lambda)-b_{n-1}Q_{n-1}(\lambda)K_\infty(\lambda)}{P_n(\lambda)-b_{n-1}P_{n-1}(\lambda)K_\infty(\lambda)}. \tag{6}$$

The functions $P_n(\lambda)$ are polynomials of degree n which satisfy the recurrence relation

$$b_nP_{n+1}(\lambda)=(\lambda-a_n)P_n(\lambda)-b_{n-1}P_{n-1}(\lambda) \tag{7}$$

for the initial conditions

$$P_{-1}(\lambda)=0;\quad P_0(\lambda)=1; \tag{8}$$

$Q_n(\lambda)$ are polynomials of degree $n-1$ which satisfy the same recurrence relation (7) but for the initial conditions

$$Q_0(\lambda)=0;\quad Q_1(\lambda)=b_0^{-1}. \tag{9}$$

Here a_n and b_n are, respectively, the diagonal and off-diagonal elements of the tridiagonal Jacobi (J) matrix of the operator induced by operator (3) in the given subspace. $K_\infty(\lambda)$ is the function to which the continued fraction corresponding to the J matrix contracts when all its elements are equal to their limiting values. If the continuum band of the crystal is simply connected, $\lambda\in[0,\lambda_m]$, then

$$\lim_{n\to\infty}a_n=2\lim_{n\to\infty}b_n=\frac{\lambda_m}{2}, \tag{10}$$

and the function $K_\infty(\lambda)$ has the form

$$K_\infty(\lambda)=\frac{4}{\lambda_m^2}\{2\lambda-\lambda+2Z(\lambda)\sqrt{\lambda|\lambda-\lambda_m|}\}, \tag{11}$$

$$Z(\lambda)\equiv i\Theta(\lambda)\Theta(\lambda_m-\lambda)-\Theta(\lambda-\lambda_m). \tag{12}$$

The function $G_{(n)}(\lambda)$ is a certain approximation of the Green function, its accuracy being determined by the value of n (the order of the Huygens wavelet) and the rate of convergence of the matrix elements to their limiting values (10) with increasing n.

Any element of the Green operator $G_{mn}(\lambda)$ is related to the Green function by the simple relation

$$G_{mn}(\lambda)=-P_m(\lambda)Q_n(\lambda)+P_m(\lambda)P_n(\lambda)G(\lambda);\quad (m\leqslant n). \tag{13}$$

Thus expressions (6)–(13) completely specify a scheme for evaluation of the Green operator of the system.

The unit-normalized spectral density

$$\rho_{(n)}(\lambda)=\frac{1}{\pi}\operatorname{Im}G_{(n)}(\lambda)$$

$$=\frac{8}{\pi\lambda_m^2}\frac{\sqrt{\lambda(\lambda_m-\lambda)}}{|P_n(\lambda)-b_{l-1}P_{n-1}(\lambda)K_\infty(\lambda)|^2}\cdot\Theta(\lambda)\Theta(\lambda_m-\lambda) \tag{14}$$

is the so-called *regular* or *elliptical* distribution of the squares of the frequencies (often used in approximate calculations; see, e.g., Ref. 19), modulated by a certain polynomial of degree $2n$. It is easy to see that both the function (14)

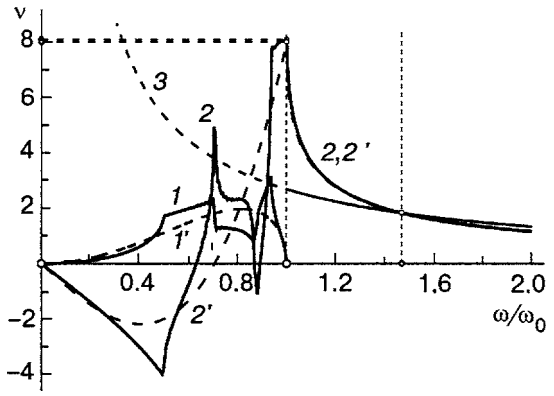

FIG. 1. Spectral densities (curves *1* and *1′*) and the real parts of the Green functions (*2* and *2′*) of the ideal fcc crystal lattice with a central interaction of the nearest neighbors. The point of intersection of curves *2* and *3* determines the local frequency; curves *2′* and *3* are its approximation with the use of the function $G_{(1)}(\omega)$.

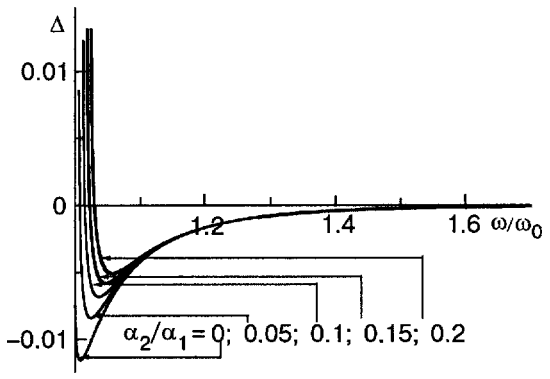

FIG. 3. Evolution of the frequency dependence $\Delta(\omega)$ with increasing interaction with next-nearest neighbors (α_1 and α_2 are the force constants of the first and second neighbors, respectively).

and the approximation of the real part of the Green function which follows from Eq. (6) are analytic inside the continuum band. Such an approximation of the real and imaginary parts of the Green function cannot be their exact expression, since the given functions are not analytic in the continuum band. Although even at relatively modest values of n the real and imaginary parts of (6) on the intervals of regularity of the real and imaginary parts of the function $G(\lambda)$ converge to the true values of these functions, near singular points (Van Hove singularities) the deviation of (14) and (6) from those true values are noticeable even at relatively large values of n (see, e.g., Ref. 20).

Outside the continuum band the behavior of the Green function is substantially simpler. For $\lambda > \lambda_m$ the function $G(\lambda) \equiv \mathrm{Re}\, G(\lambda)$ and can be expressed in terms of an integral of the spectral density. The singularities will be smoothed out, and outside the continuum band the Green function will be analytic.

The rate of convergence of this function with increasing n is very high—the approximations (6) for $n=1$ and large n coincide to a high accuracy, as is clearly seen in Figs. 1 and 2. Figure 1 shows the dependence and frequency ω of the real part of the Green function $G_{(n)}(\omega) \equiv 2\omega G_{(n)}(\lambda)$ (curves *2* and *2′*) and also the corresponding spectral density $\nu(\omega) = \pi^{-1}\,\mathrm{Im}\, G(\omega)$ (curves *1* and *1′*) for an fcc crystal lattice

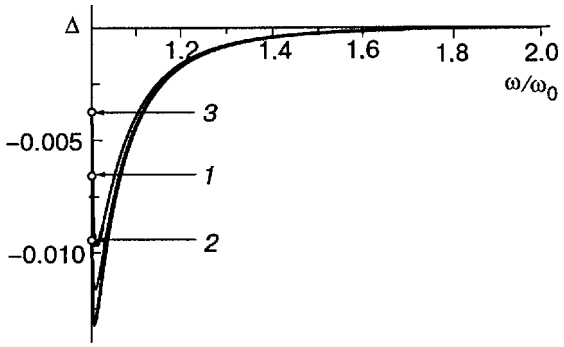

FIG. 2. Frequency dependence of the relative deviation Δ of the approximation $G_{(1)}(\omega)$ from the function $G_{(60)}(\omega)$ for ideal crystal lattices with a central interaction of nearest neighbors: fcc (*1*), hcp, for displacement along the a axis (*2*); hcp, for displacement along the c axis (*3*).

with a central interaction between nearest neighbors. Curves *1* and *2* correspond to $n=60$ for the fcc case and to $n=36$ for the hcp, while the primed curves *1′* and *2′* correspond to $n=1$. The spectral densities $\rho(\omega)$ are normalized to unity, while the normalization of $\mathrm{Re}\, G(\omega)$ is determined by the Kramers-Kronig relation. Although for $\omega \in [0, \omega_m]$ the curves calculated for $n=1$ and large n have little in common, for $\omega > \omega_m$ the curves *2* and *2′* practically merge, except in a very narrow region near the boundary of the continuum band.

Figure 2 shows, for frequencies $\omega \geqslant \omega_m$, the frequency dependence of Δ, defined as

$$\Delta \equiv \frac{G_{(1)}(\omega) - G_{(60)}(\omega)}{G_{(60)}(\omega)},$$

i.e., the relative deviation of the approximation of the function $G_{(60)}(\omega)$ by $G_{(1)}(\omega)$, for an ideal crystal lattice with a central interaction of nearest neighbors: fcc (curve *1*) and hcp for the case $c/a = \sqrt{8/3}$ (curves *2* and *3*, for the generating displacement directed along the a and c axes, respectively). It is seen that Δ varies from values of $\sim 1\%$ near the boundary of the continuum band to values ~ 0.1–0.01% at appreciable distances from it.

To determine the local frequency due to the presence of a light isotopic substitutional impurity in the crystal, one can write the Lifshits equation (4) in the form

$$G(\omega) \equiv S(\omega, \hat{\Lambda}) = \frac{2}{\varepsilon\omega}, \tag{15}$$

where ε is the mass defect of the impurity atom:

$$\varepsilon \equiv \frac{\Delta m}{m} = \frac{m' - m}{m} \tag{16}$$

(m' and m are the masses of the impurity and host atoms, respectively). Figure 1 shows an example of the graphical solution of the Lifshits equation (15). Curve *3* in this figure corresponds to the function $S(\omega, \varepsilon)$ for $\varepsilon = -0.75$ (the impurity atom is one-fourth as heavy as the host atom). The values of ω at which this curve intersects the curves of $G_{(60)} \times(\omega)$ and $G_{(1)}(\omega)$ (i.e., the values of the corresponding local frequencies) agree to within $\sim 10^{-4}$.

As can be seen in Fig. 3, taking the interaction with more remote neighbors into account does not degrade (and,

near the boundary of the continuous spectrum, even improves) the accuracy of approximation of the Green function by $G_{(1)}(\omega)$ for $\omega \geqslant \omega_m$. Thus in this case the given approximation is entirely suitable for describing the characteristics of the local modes.

We note that it is straightforward to obtain analytical expressions both for the first matrix elements a_0 and b_0 of the J matrix and for the function $G_{(1)}(\lambda)$. Therefore, the fact that outside the continuum band the function $G_{(1)}(\lambda)$ is a good approximation of the Green function permits a substantial advance in the study of the local levels; in particular, it allows one to write relatively uncomplicated analytical expressions for the frequency and other characteristics of the local modes.

B. Local modes in the *J* matrix method

If the operator $\hat{\Lambda}$ in a cyclic subspace under consideration is represented by a J matrix of finite rank, then one can write the Lifshits equation[20,30,31] in that subspace and from it determine the conditions of formation and the characteristics of the local modes (see, e.g., Ref. 24).

In a number of cases a constructive alternative to the given method is to find the poles of the Green function of the *perturbed* system, when $G(\lambda) \equiv G_{00}(\lambda) = (\vec{h}_0, [\lambda \hat{I} - \hat{L}_0 - \hat{\Lambda}]^{-1} \vec{h}_0)$, i.e., when the J matrix of the operator $\hat{L} = \hat{L}_0 + \hat{\Lambda}$ is used in Eq. (6). This method is also suitable for determining the local modes due to a nondegenerate perturbation operator (if the perturbation does not alter the width of the continuum band, i.e., the limiting values of the J matrix, and can be considered "asymptotically degenerate"). The poles λ_d of the Green function determine the discrete frequencies (in particular, the local modes), and the residues at them, $\mu_0^{(d)} \equiv \mathrm{res}_{\lambda=\lambda_d} G_{00}(\lambda)$ their *intensities*, i.e., they characterize the value of the amplitude of the same modes, determined by the vector $\vec{h}_0$, at discrete frequencies, and

$$\int_0^{\lambda_m} \rho(\lambda) d\lambda + \sum_d \mu_0^{(d)} = 1.$$

It follows from Eq. (13) that $\mu_n^{(d)} \equiv \mathrm{res}_{\lambda=\lambda_d} G_{nm}(\lambda) = \mu_0^{(d)} P_n^2(\lambda_d)$, i.e., the function $P_n^2(\lambda_d)$ determines the attenuation of the amplitude of the local mode with increasing number of the secondary Huygens wavelet. When the matrix elements of the J matrix approach their limiting values (10) the sequence $\{P_n^2(\lambda_d)\}_{n=n_a}^{\infty}$ tends toward an infinitely decaying geometric progression, and thus the amplitudes of the local modes are damped exponentially.[25–27] Of course, for any local level it is necessary to satisfy the condition

$$\sum_{n=0}^{\infty} \mu_n^{(d)} = \mu_0^{(d)} \sum_{n=0}^{\infty} P_n^2(\lambda_d) = 1, \tag{17}$$

which follows from the formulas for the difference of the traces of the perturbed and unperturbed operators.[5,20,21] Thus, outside the continuum band the function $G_{(1)}(\lambda)$ is a good approximation of the Green function, and thus it is reasonable to expect that it can be used to obtain a completely satisfactory description of the characteristics of the local modes. Let us calculate these characteristics.

We introduce the parameters η and β characterizing the deviation of the matrix elements a_0 and b_0 from the limiting values (10):

$$a_0 = \frac{\lambda_m}{2(1+\eta)}; \quad b_0 = \frac{\lambda_m}{4\sqrt{1+\beta}}, \tag{18}$$

and obviously $\eta, \beta \in [-1, +\infty)$.

The Green function $G_{(1)}(\lambda)$ can be written in the form

$$G_{(1)}(\lambda) = G_{(1)}(\lambda, \eta, \beta) = \frac{4(1+\eta)(1+\beta)}{2\lambda(1+\eta)(1+2\beta) - \lambda_m(1+2\beta-\eta) - 2Z(\lambda)(1+\eta)\sqrt{\lambda|\lambda-\lambda_m|}}. \tag{19}$$

The values $\lambda = \lambda_d(\eta, \beta) > \lambda_m$ at which the denominator of Eq. (19) goes to zero determine the squares of the local mode frequencies. It follows from elementary but awkward calculations that there is one such value:

$$\lambda_1(\eta, \beta) \equiv \omega_l^2(\eta, \beta) = \frac{\lambda_m}{4\beta(1+\eta)} \left\{ 2\beta - \eta - \sqrt{-\beta + \frac{(\eta-\beta)^2}{1+\beta}} \right\} \tag{20}$$

which exists for

$$\begin{cases} \beta < -\dfrac{3}{4}; \\ \eta \in [-1, +\infty); \end{cases} \quad \text{or} \quad \begin{cases} \beta > -\dfrac{3}{4}; \\ \eta < \eta^*\beta) \equiv -\dfrac{1+2\beta}{3+4\beta} \end{cases}. \tag{21}$$

The shaded region in Fig. 4 corresponds to the presence of local modes in a system characterized by parameters η and β.

It was shown in Ref. 24 that the threshold values of the parameters η and β, which lie on the curve $\eta = \eta^*(\beta)$, correspond to a square-root singularity of the spectral density at $\lambda = \lambda_m$. Indeed, the spectral density

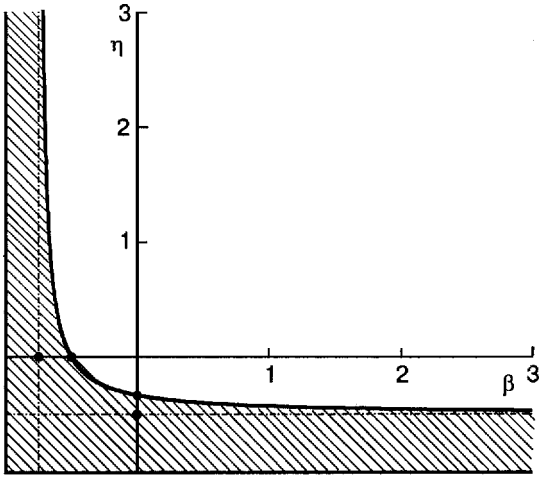

FIG. 4. Regions of the existence (shaded) and absence of local modes in a system described by the Green function (19). The separating curve $\eta = \eta^*(\beta)$ is determined by the system of inequalities (21).

$$\rho_{(1)}(\lambda,\eta,\beta) = \frac{1+\eta}{4\pi\beta}\frac{\sqrt{\lambda(\lambda_m-\lambda)}}{\prod_{d=1}^{2}(\lambda-\lambda_d)}, \tag{22}$$

where λ_2, which differs from λ_1 by the sign in front of the radical in the definition (20), has the same singularity at $\eta = \eta^*$, since there $\lambda_1 = \lambda_m$. In particular, the *ideal* linear chain with nearest-neighbor interactions corresponds to $\eta = 0$ and $\beta = -1/2$. These values lie on the curve $\eta = \eta^*(\beta)$. The spectral density of such a chain has square-root features at the edges of the continuum band, and the formation of local modes of a light or strongly coupled impurity occurs in a thresholdless manner.

For the local-mode intensity $\mu_0 = \mathrm{res}_{\lambda=\omega_l^2} G(\lambda)$ we obtain

$$\mu_0 = \frac{1+\eta}{4\beta(\lambda_1-\lambda_2)}\left\{2\lambda_1(1+2\beta) - \lambda_m\frac{1+2\beta-\eta}{1+\eta} - 2\sqrt{\lambda_1(\lambda-\lambda_m)}\right\}$$
$$= \frac{\eta+(1+2\beta)\sqrt{-\beta+\dfrac{(\eta-\beta)^2}{1+\beta}}}{2\beta\sqrt{-\beta+\dfrac{(\eta-\beta)^2}{1+\beta}}}\left\{\Theta\left(-\frac{3}{4}-\beta\right)+\Theta\left(\beta+\frac{3}{4}\right)\Theta\left(-\frac{1+2\beta}{3+4\beta}-\eta\right)\right\}. \tag{23}$$

Substituting (20) into the Lifshits equation,[20,24] which for the system under discussion has the form ($\lambda \notin [0, \lambda_m]$),

$$\lambda_m + 2\left[\beta(2\lambda-\lambda_m) + \lambda_m\frac{1+\beta}{1+\eta}\right][2\lambda-\lambda_m-2\sqrt{\lambda(\lambda-\lambda_m)}] = 0, \tag{24}$$

shows that $\lambda_1(\eta,\beta)$ satisfies this equation when conditions (21) hold.

It was mentioned above that as a measure of the attenuation of the modes one can use the change of the mode amplitude with increasing number n of the secondary Huygens wavelet, and that change is proportional to $P_n^2(\lambda_1)$. Substituting Eq. (20) into (7) and (8), we obtain

$$P_1(\lambda_1) = -\frac{\sqrt{1+\beta}}{\beta(1+\eta)}\left[\eta + \sqrt{-\beta+\frac{(\eta-\beta)^2}{1+\beta}}\right]. \tag{25}$$

It is easy to prove by mathematical induction that for $n \geqslant 1$

$$P_n(\lambda_1) = \frac{1}{\sqrt{1+\beta}}[\sqrt{1+\beta}P_1(\lambda_1)]^n, \tag{26}$$

and consequently, the values of μ_n, provided they are nonzero (i.e., if conditions (21) hold, and the local levels actually exist), for $n \geqslant 1$ form a geometric progression:

$$\mu_n = \mu_1 q^{n-1} = \frac{\mu_0}{1+\beta}q^n. \tag{27}$$

The denominator of this progression,

$$q = [\sqrt{1+\beta}\,P_1(\lambda_1)]^2 = \left\{\frac{(1+\beta)}{\beta(1+\eta)}\left[\eta+\sqrt{-\beta+\frac{(\eta-\beta)^2}{1+\beta}}\right]\right\}^2 \tag{28}$$

under condition (21) is less than unity, and condition (17) holds.

Thus the formulas obtained in this Section, Eqs. (20), (21), (23), and (28), contain a complete solution of the problem of atomic dynamics for local modes in a system described by the Green function (19), i.e., they determine the existence conditions of the local modes and their frequency, intensity, and damping. In the next Section we analyze and illustrate the applicability of these results for specific models of close-packed crystals containing substitutional impurities.

II. LOCAL MODES DUE TO THE PRESENCE OF A SUBSTITUTIONAL IMPURITY IN CLOSE-PACKED CRYSTAL LATTICES

In the previous Section we considered the Green function of the perturbed system [Eq. (19)], although nonzero parameters η and β can also exist for a defect-free structure and, to a first approximation, can characterize the features of its geometry and interaction force. For a lattice containing

defect atoms the parameters η and β will be some functions of the parameters of the defect—the relative changes of the mass, ε [Eq. (16)], and of the force constant of the interaction, γ:

$$\gamma \equiv \frac{\Delta\alpha}{\alpha} = \frac{\alpha' - \alpha}{\alpha}, \tag{29}$$

where α' and α are the force constants describing the interaction of an impurity with the nearest neighbors and the interatomic interaction in the ideal lattice. The values of the functions $\eta(\varepsilon,\gamma)$ and $\beta(\varepsilon,\gamma)$ for which the influence of the defect vanishes can be nonzero (as we have said, the ideal linear chain corresponds to $\beta=-1/2$). However, the defect-free system cannot correspond to values of η and β corresponding to the presence of local modes (see, e.g., Ref. 32). In particular, for ideal lattices the inequality $\beta>-3/4$ should hold.

After determining the functions $\eta(\varepsilon,\gamma)$ and $\beta(\varepsilon,\gamma)$ for specific crystal structures with different defect configurations and substituting them into Eqs. (20), (23), (28), and (21), one can obtain the dependence of the conditions of formation and the dynamic characteristics of local modes on the parameters characterizing the individual defect, the configuration of defects, and also the ideal lattice. In this Section we obtain these dependences for substitutional impurities in fcc and hcp lattices. The results are compared with numerical calculations done with the use of J matrices of high rank.

A. Isolated isotopic impurity in fcc and hcp crystal lattices

An isotopic substitutional impurity is an important object in the dynamics of a lattice with defects. This is because, first, the contribution to the vibrational spectrum of the crystal introduced by real substitutional impurities (the kind most often encountered) is mainly due to the mass difference, and some solid solutions can to sufficient accuracy be treated as isotopic (e.g., Ag–Al).[2)] Second, if the chemical composition of the solution is known, then the mass difference of the host and impurity is known precisely, and the difference of the force constants and the values of the stresses due to the presence of the impurity and the influence of other processes (rotation, conversion) are the direct problem of the experiment. To solve this problem, one must compare the experimental data with the theoretical calculation for an isotopic impurity model, and that makes a theoretical account of the influence of the isotope effect an inescapable part of the experimental research.

The cyclic subspaces generated by displacements of an isolated isotopic impurity along the principal crystallographic axes contains complete information about the change of the phonon spectrum of the crystal due to such a defect.[20,30,31] In each such subspace there are only two nonzero elements of the J matrix of the perturbation operator $\hat{\Lambda}$:

$$\Lambda_{00} = -\frac{\varepsilon}{1+\varepsilon}a_0, \quad \Lambda_{01} = \left(1 - \frac{1}{\sqrt{1+\varepsilon}}\right)b_0, \tag{30}$$

where ε is the mass defect (16), and a_0 and b_0 are the first two elements of the J matrix of the *unperturbed* operator. Consequently, the parameters η and β (18) completely describe the perturbation introduced by such a defect.

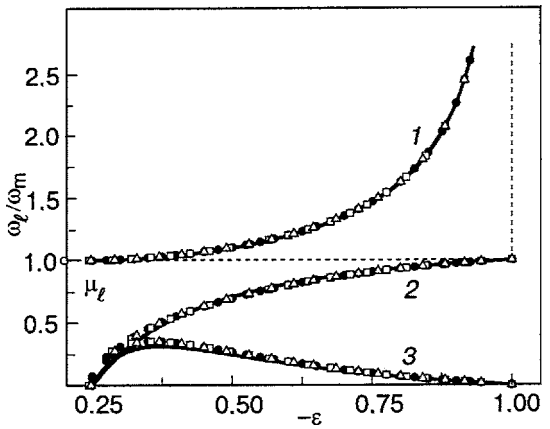

FIG. 5. Plots of the main characteristics of the local mode due to an isolated isotopic impurity in close-packed crystal lattices with a central interaction of nearest neighbors versus the mass defect. The local mode frequency (*1*), the local mode intensity at the impurity atom itself (*2*), and the local mode intensity at the first coordination sphere of the impurity (*3*). The solid curves are calculated using a J matrix of the first rank; the data points are calculated using a J matrix with $n=60$: ●—fcc; □ and △—hcp, along the a and c axes, respectively.

The force matrices $\Phi_{ik}(\Delta)$ for the case of a central interaction between atoms have the form

$$\Phi_{ik}(\Delta) = -\alpha(\Delta)\frac{\Delta_i\Delta_k}{\Delta^2}(1-\delta_{\Delta,0}) + \delta_{\Delta,0}\sum_{\Delta}\alpha(\Delta)\frac{\Delta_i\Delta_k}{\Delta^2}. \tag{31}$$

In this study we limit consideration to the nearest-neighbor interaction. Let us first consider fcc and hcp crystal structures with $\kappa=1$. Then all of the values of Δ are identical, and $\alpha(\Delta)\equiv\alpha$. Then the square of the maximum frequency is $\lambda_m=8\alpha/m$. The matrix elements $a_0=\lambda_m/2$ and $b_0=\lambda_m/4$, i.e., the Green function (19) coincides with the quantity $K_\infty(\lambda)$ determined in Eq. (11).

In cyclic subspaces generated by displacements of an isotopic impurity, the parameters $\eta=\beta=\varepsilon$. Substituting these values into (20), (23), and (29), we obtain

$$\omega_l^2 = \left(\frac{\omega_m}{2}\right)^2 \frac{1}{\sqrt{|\varepsilon|}(1-\sqrt{|\varepsilon|})}; \tag{32}$$

$$\mu_0 = 1 - \frac{1-\sqrt{|\varepsilon|}}{2|\varepsilon|}\cdot\Theta\left(-\frac{1}{4}-\varepsilon\right); \tag{33}$$

$$q = \left(\frac{1-\sqrt{|\varepsilon|}}{\sqrt{|\varepsilon|}}\right)^2. \tag{34}$$

Figure 5 shows plots of $\omega_l(\varepsilon)$ and $\mu_0(\varepsilon)$ and also of the quantity

$$\mu_l(\varepsilon) = \mu_0(\varepsilon)P_1^2(\omega_l^2) = \left(\sqrt{|\varepsilon|}-\frac{1}{2}\right)\left(\frac{1-\sqrt{|\varepsilon|}}{\varepsilon^2}\right)\Theta\left(-\frac{1}{4}-\varepsilon\right), \tag{35}$$

calculated according to formulas (32)–(35) and also with the Green function (6) obtained using J matrices of high rank. Only near the boundary of the continuous spectrum is there a

TABLE I. Values of $G_{00}(\omega_m+0)$ and the threshold values of the mass defect for fcc and hcp ($\kappa=1$) crystal lattices.

System	$G_{00}(\omega_m+0)$	ε^*
J matrix of rank n=1	8	−0,25
fcc	8.161155	−0.245063
hcp [100]	8.214850	−0.243462
hcp [001]	8.080908	−0.247497

noticeable ($\sim 5\%$) difference in the behavior of the intensities (but not frequencies) of the local modes.

We note that already for $\omega_l \gtrsim 1.01\omega_m$ the quantity $1-[\mu_0(\varepsilon)+\mu_l(\varepsilon)] \lesssim 10^{-4}$, i.e., the local mode is almost completely localized within the first coordination sphere of the impurity atom.

The value of the threshold mass defect ε^* necessary for the local mode to arise can be determined from the condition that the Lifshits equation hold for $\lambda \to \lambda_m+0$. In Ref. 24 it was shown that

$$\varepsilon^* = \frac{1}{\lambda_m G(\lambda_m+0)} = \frac{2}{\omega_m G(\omega_m+0)}. \tag{36}$$

The values of $G(\omega_m+0)$ and ε^* for the systems considered are presented in Table I.

If in the hcp crystal lattice the parameter $\kappa \neq 1$, then $\alpha(\Delta)=\alpha\delta_{\Delta_{z,0}}+\alpha_c(1-\delta_{\Delta_{z,0}})$, where $\alpha \equiv \alpha(a)$, $\alpha_c \equiv \alpha(a\sqrt{(1+2\kappa^2)/3})$ (a is the hcp lattice constant). If the maximum frequency is reached at the bottom of the optical band, as is typically the case in the majority of such structures, then, in the cyclic subspaces generated by displacements of the impurity along and perpendicular to the c axis, the parameters η and β can be represented in the form

$\vec{h}_0 = |0|[100]\rangle$:

$$\eta(\varepsilon) = \frac{\alpha_c[4\kappa^2(1+\varepsilon)-1]-3\alpha}{\alpha_c+3\alpha};$$

$$\beta(\varepsilon) = \frac{\alpha_c^2\kappa^2[2\kappa^2(5+6\varepsilon)-1]-9\alpha^2}{\alpha_c^2\kappa^2(1+2\kappa^2)+9\alpha^2};$$

$\vec{h}_0 = |0|[001]\rangle$:

$$\eta(\varepsilon) = \varepsilon; \quad \beta(\varepsilon) = \frac{-1+\kappa^2(1+3\varepsilon)}{1+2\kappa^2}. \tag{37}$$

The substitution of these parameters into Eqs. (20), (23), and (28) leads to straightforward but very awkward calculations for the characteristics of the local modes, and we see no point in writing them out in explicit form.

A comparison of the results obtained in that way with the results of a calculation with Green functions obtained using J matrices of high rank is presented in Fig. 6. It is seen than in that case Eq. (20) is a very good approximation of the local frequency in the entire frequency range, and that Eq. (23) describes the intensity of the local mode well for $\omega_l \gtrsim 1.05-1.10\omega_m$. In practice, for determining the characteristics of a local vibrational mode it is sufficient to take into consideration that the spectral density near ω_m has a definite shape: $\rho(\lambda) \sim \sqrt{\omega_m^2-\omega^2}$ (see, e.g., Ref. 7). Such an approximation of the spectral density was used, in particular, in Ref. 33. The coefficient of proportionality can be expressed in terms of the mean frequency and its variance over the spectrum, and, hence, in terms of a_0 and b_0. Indeed, since the polynomials $P_n(\lambda)$ are orthonormalized in the Hilbert space with a weight factor $\rho(\lambda)$ (see, e.g., Refs. 28 and 29, one has

$$a_0 = M_1; \quad b_0 = \sqrt{M_2 - M_1^2}, \tag{38}$$

where $M_n \equiv \int_0^\infty \lambda^n \rho(\lambda) d\lambda$. Accordingly, the matrix element a_0 is the square of the Einstein frequency, and the matrix element b_0 characterizes the variance of the mode distribution.

The values of a_0 and b_0 are influenced only by those neighbors of the impurity atom with which it directly interacts. In the model considered here these are the nearest neighbors, and therefore the possibility of describing the local frequencies to high accuracy with the use of Eq. (20) means that the other perturbations acting on the lattice have practically no effect on the local mode frequency if they do not touch the first coordination sphere of the impurity. In particular, at a finite concentration of impurity atoms the smearing of the local levels occurs mainly on account of impurity pairs in positions such that there is an intersection of the sets of atoms with which each member of the pair interacts. This case is considered in the next subsection.

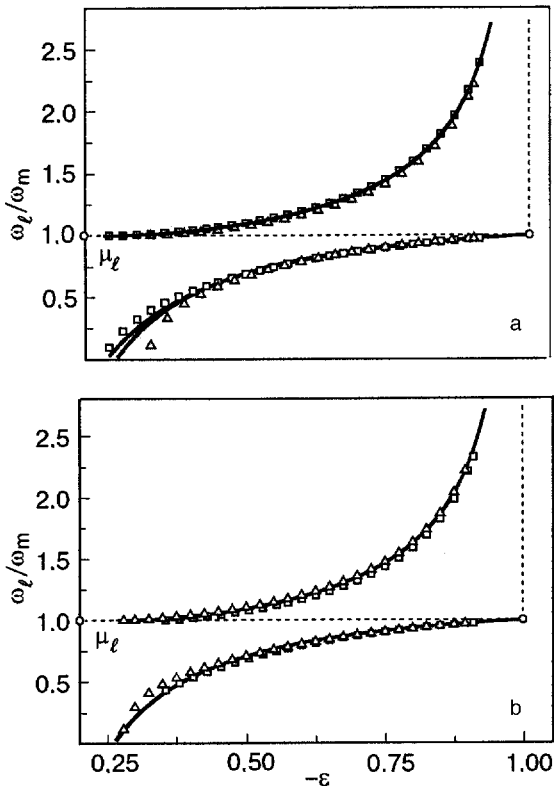

FIG. 6. Plots of the frequency and intensity of the local mode due to the presence of an isolated isotopic impurity in an hcp crystal lattice with a central interaction of nearest neighbors versus the mass defect for nonzero values of the parameters $\kappa \equiv a/c\sqrt{8/3}$: $\kappa=1.05$, $\alpha_c=0.88\alpha$ (a); $\kappa=0.95$, $\alpha_c=1.15\alpha$ (b). The solid curves are the result of a calculation using a J matrix of the first rank, □ and △ using a J matrix with $n=60$ (along the perpendicular to the c axis).

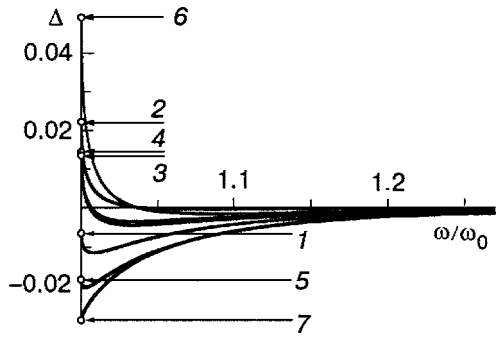

FIG. 7. Frequency dependence of Δ for an isolated defect in the form of a pair of adjacent impurities introduced into an ideal fcc crystal lattice with a central interaction of nearest neighbors: the displacement τ_-^5 (one of the isolated impurities is displaced in an arbitrary direction) (*1*); τ^8 (*2*); τ^6 (*3*); τ^1 (*4*); τ^7 (*5*); τ^4 (*6*) (the generating vectors are given in the Appendix).

B. Local modes due to a pair of isotopic impurities in an fcc lattice

In an fcc crystal lattice with a central interaction between nearest neighbors there will be atoms interacting with both impurities if the impurities are nearest, next-nearest, third-nearest, or fourth-nearest neighbors of each other.

Suppose there is an isolated pair of isotopic impurities that are nearest neighbors of each other. We place the origin of the coordinate system at one of the impurities and choose the coordinate axes to lie along the fourfold axes in such a way that the coordinates of the other impurity are $(a/2,a/2,0)$, where a is the fcc lattice constant.

Unlike the case of a single isolated impurity, the presence of such a defect lowers the symmetry of the system from O_h to D_{2h}. The whole space of atomic displacements can be represented in the form a direct sum of six mutually orthogonal cyclic subspaces, each of which transforms according to a one-dimensional irreducible representation of the point group D_{2h}: τ^i ($i=1,3,4,5,6,8$ in the notation of Ref. 34). Each of these cyclic subspaces is generated by a simultaneous displacement of nearest neighbors of the atoms (in-phase or antiphase) in the direction along the straight line joining these atoms (τ^1 and τ^8) and in the two directions perpendicular to that straight line. Each of the six different operators $\hat{L}_0^{(i)}$ induced in these subspaces by the operator $\hat{L}_0$ describing the modes of the ideal crystal will suffer a perturbation due to isotopic substitution which is given by expressions (30), where a_0 and b_0 are the first two elements of the J matrix of the corresponding operator. Thus one can determine the values of $\eta(\varepsilon)$ and $\beta(\varepsilon)$ in each of the cyclic subspaces τ^i [they are given in formulas (A1)–(A6) of the Appendix].

In each of the cyclic subspaces τ^i the Green function outside the continuum band, as is seen in Fig. 7, is well approximated by expression (19) in which the parameters η and β are replaced by the values $\eta(0)$ and $\beta(0)$ from Eqs. (A1)–(A6).

Substitution of the corresponding values of $\eta(\varepsilon)$ and $\beta(\varepsilon)$ into Eqs. (20), (23), and (28) gives analytical expressions for the frequencies, intensities, and damping parameters of the local modes, also given in Eqs. (A1)–(A6). Figure 8 shows the dependence of the frequencies and intensities of the local modes in each of the cyclic subspaces,

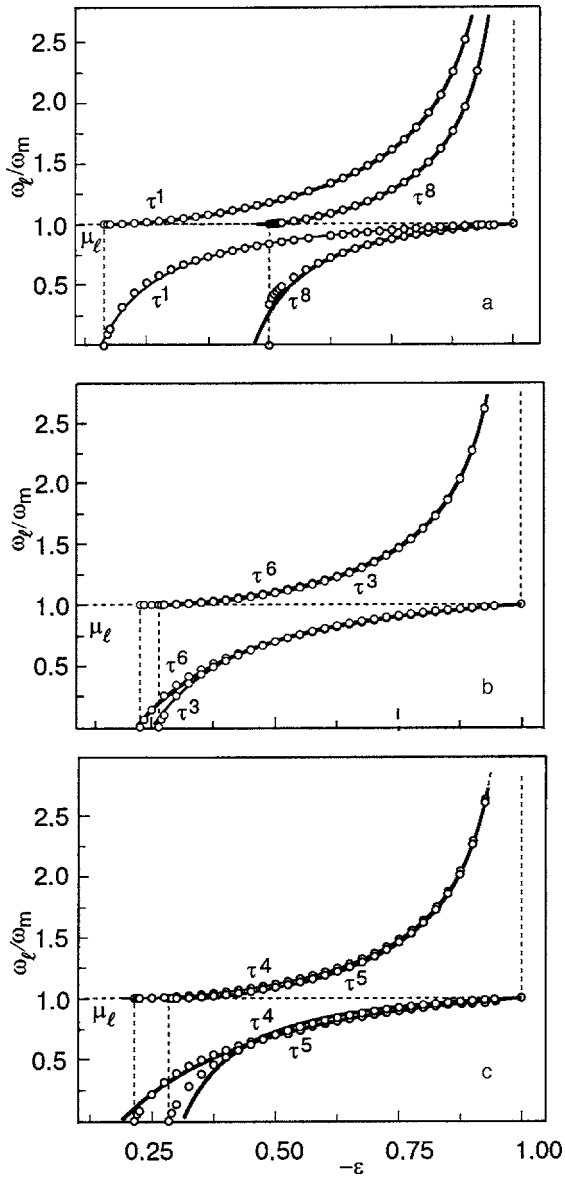

FIG. 8. Plots of the frequencies and intensities of local modes of an isolated pair of adjacent isotopic impurities in an fcc crystal lattice with a central interaction of nearest neighbors versus the mass defect. The solid curves are calculated using a J matrix of the first rank, and the curves are calculated using a J matrix with $n=60$.

calculated both according to formulas (A1)–(A6) and with the use of the Green functions recovered from the J matrices of rank $n=50$. As in the previous cases, the difference is noticeable only in the behavior of the intensities for modes with frequencies just slightly above ω_m.

The term describing the contribution of an isotopic defect in the Lifshits equation is independent of the parameters of the ideal lattice and is the same in all the cyclic subspaces.[24] Therefore for determining the thresholds for the appearance of local modes in each of the subspaces τ^i one can use relation (36) with the Green function of the ideal lattice in the given subspace. The values of $G(\omega_m)$ and the threshold values of the mass defect are presented in Table II.

The maximum distance between local mode frequencies at a fixed value of ε in the different cyclic subspaces, i.e., the difference $\Delta\omega_l(\varepsilon)=\omega_l^{(\tau^1)}(\varepsilon)-\omega_l^{(\tau^8)}(\varepsilon)$, can serve as an estimate of the width of the impurity band at finite impurity

TABLE II. Values of $G_{00}(\omega_m+0)$ and the threshold values of the mass defect for an fcc lattice.

$H^{(i)}$	$G_{00}(\omega_m+0)$		ε^*	
	$n=50$	$n=1$	$n=50$	$n=1$
τ^1	12.30378	12.8	−0.162552	−0.15625
τ^3	7.562446	$\frac{64}{9}$	−0.264465	−0.28125
τ^4	9.315600	$\frac{32}{3}$	−0.214694	−0.18750
τ^5	7.039269	6.4	−0.284120	−0.31250
τ^6	8.817075	$\frac{64}{7}$	−0.226833	−0.21875
τ^8	4.000041	$\frac{64}{15}$	−0.499995	−0.46875

concentrations c. For the case considered in this Section, an fcc crystal lattice with a central interaction between nearest neighbors, in the subspace generated by the displacements of any atom, the displacements of its next-nearest neighbors do not appear in the basis vectors $\vec{h}_1,\vec{h}_2$, i.e., they do not contribute to the matrix elements a_0 and b_0 nor to the two first moments of the spectral density. Therefore, if two isotopic impurities are next-nearest neighbors of each other, then the characteristics of the local modes for such a pair of impurities will be described by expressions (32)–(34), although there is an intersection of the sets of atoms with which each of them interacts. Taking into account a next-nearest-neighbor interaction or a noncentral interaction between nearest neighbors will lift the degeneracy of the local modes, which, as in the case of impurity atoms located next to each other, become dependent on their mutual displacements.

For pairs of impurities which are third- and fourth-nearest neighbors of each other, the interaction between impurities affects only the matrix element b_0 (as in the subspaces τ^2-τ^6 for a pair of adjacent impurities). If the impurities are fourth-nearest neighbors of each other, the interaction will lead only to displacements along the line connecting them, and in that case the dependence on the mass defect of the parameters η and β and, hence, of all the characteristics of the local modes is identically equal to the analogous dependence in the subspace τ^4 for the in-phase displacement and in the subspace τ^5 for the antiphase displacement [see Eqs. (A3) and (A4), respectively, in the Appendix].

Analytical expressions for the parameters η and β as functions of the mass defect ε and also for the existence conditions and the main characteristics of the local modes are given in formulas (A7)–(A13), respectively.

C. Local modes due to light, weakly coupled impurities

In many cases, for different elements forming identical crystal lattices (e.g., an fcc lattice) the lighter atoms have smaller atomic radii and lattice constants (see, e.g., Table III). Therefore a light substitutional impurity will often be going into a lattice with an interatomic distance Δ exceeding Δ_0, the distance corresponding to the minimum of the characteristic interatomic interaction potential for the given impurity atom. This, as a rule, will lead to weakening of the coupling of the impurity with its environment. Strictly speaking, noncentral forces should arise, but straightforward estimates (given, e.g., in Ref. 36) show that in the region of Δ values in which the existence of local modes is still possible, the noncentral forces are negligible, and the interatomic interaction can be considered central.

TABLE III. Atomic masses, atomic radii, and lattice constants of solidified rare gases.[35]

	m, at. units	σ, Å	a, Å
Ar	39.94	3.405	5.40
Kr	83.80	3.624	5.59
Xe	131.30	3.921	6.20

The problem of the conditions of formation and characteristics of the local modes in an fcc crystal lattice containing impurities that differ in both mass and interatomic interaction is considered in Ref. 24. As in the case of a light isotope, the local modes due to a light, weakly coupled impurity arise only in the cyclic subspace generated by the displacement of the impurity atom itself. This subspace transforms according to the irreducible representation τ^5 of the point group O_h (in the notation of Ref. 34).

The perturbation operator $\hat{\Lambda}$ in this subspace has three nonzero matrix elements:[20,30,31]

$$\Lambda_{00}=\frac{-\varepsilon+\gamma}{1+\varepsilon}a_0;\quad \Lambda_{01}=\left(1-\frac{1+\gamma}{\sqrt{1+\varepsilon}}\right)b_0,\quad \Lambda_{01}=\gamma\frac{\lambda_m}{8}, \tag{39}$$

and a given perturbation cannot be described in terms of the parameters η and β. However, because the J matrix of an ideal fcc lattice has the matrix element $a_1=9/16$, when the coupling force is decreased by less than half ($-1/2\leqslant\gamma<0$) this circumstance only improves the approximation of the Green function by expression (19). For a greater weakening of the interatomic interaction the existence of local modes is improbable, but the spectral properties can still be described adequately using to the first two moments, since in that case the vibrational modes will be strongly localized (see, e.g., Ref. 37).

Using Eq. (39), we can write for the parameters η and β

$$\eta(\varepsilon,\gamma)=\frac{\varepsilon-\gamma}{1+\gamma};\quad \beta(\varepsilon,\gamma)=\frac{\varepsilon-\gamma(2+\gamma)}{(1+\gamma)^2}. \tag{40}$$

Substituting these values into (20), (23), and (28), we obtain

$$\begin{cases} \omega_l^2 = \left(\dfrac{\omega_m}{2}\right)^2 \dfrac{1-|\gamma|}{1-|\varepsilon|} \dfrac{|\varepsilon|-|\gamma|(3-|\varepsilon|-|\gamma|)+(1-|\gamma|)^{3/2}\sqrt{|\varepsilon|-|\gamma|(2-|\varepsilon|)}}{|\varepsilon|-|\gamma|(2-|\gamma|)}; \\ \mu_0 = \dfrac{\Theta\left(\dfrac{-1+4\gamma+\gamma^2}{4}-\varepsilon\right)}{2[|\varepsilon|-|\gamma|(2-|\gamma|)]\sqrt{|\varepsilon|-|\gamma|(2-|\varepsilon|)}} \{[2(1+|\gamma|)^2-2(\varepsilon|+\gamma^2)]\sqrt{|\varepsilon|-|\gamma|(2-|\varepsilon|)}+(|\varepsilon|-|\gamma|)(1-|\gamma|)^{3/2}\}; \\ q = \left\{\dfrac{|\varepsilon|-|\gamma|-\sqrt{(1-|\gamma|)|\varepsilon|-|\gamma|(2-|\varepsilon|)}}{|\varepsilon|-|\gamma|(2-|\gamma|)}\right\}^2. \end{cases} \tag{41}$$

The evolution of the local frequencies and intensities of the local modes with changing parameters γ and ε is presented in Figs. 9 and 10. As for all the cases considered in this paper, these figures compare the results (41) with calculations using a J matrix of rank $n=60$. For a light, weakly coupled impurity the agreement of the results of the two calculations is even better than for a light isotopic impurity.

CONCLUSION

Thus the analytical expressions (20), (23), and (28) obtained in the framework of the approximation of the spectral density of the crystal lattice with a simply connected quasicontinuum band according to the known first two moments and the behavior at the ends of that band describe the characteristics of the local modes due to the presence of a light impurity (isotopic or weakly coupled) in close-packed crystal structures to a high accuracy. The agreement will be better the farther the local level lies from the upper edge of the continuum band, but even near the upper boundary the agreement can be considered entirely satisfactory. In particular, the existence conditions of the local modes is described by expression (21) with an accuracy of 2–3%.

The applicability of these formulas for other structures can be determined by investigating the rate of convergence of the Green function outside the continuum band with increasing rank of the corresponding J matrix, corresponding to the approach to a spherical shape of a wave front propagating in the crystal lattice from a localized source. Good agreement of the given formulas should be expected for light isotopic and light weakly coupled impurities not only in close-packed but also other crystal lattices, including, in particular, those with multiatomic unit cells but having a simply connected continuum band and also highly anisotropic layered and "chain" crystals. As to the case of strongly coupled impurities (especially heavy ones), in the cyclic subspaces generated by displacements of the impurity atom itself the aforementioned agreement can be degraded because of the large deviation of the matrix element a_1 from its asymptotic value (connected to the third moment of the spectral density). In those cyclic subspaces in which the impurity atom is at rest and the rank of the perturbation operator $\hat{\Lambda}$ is equal to unity (see, e.g., Ref. 24), one should expect good agreement of the characteristics of the local modes with formulas (20), (21), (23), and (28).

At finite impurity concentrations the smearing of the local level will be due primarily to impurity configurations characterized by a change of the first moment of the spectral density, and in lattices with nearest-neighbor interaction—to groups of impurity atoms for which each of the atoms is a

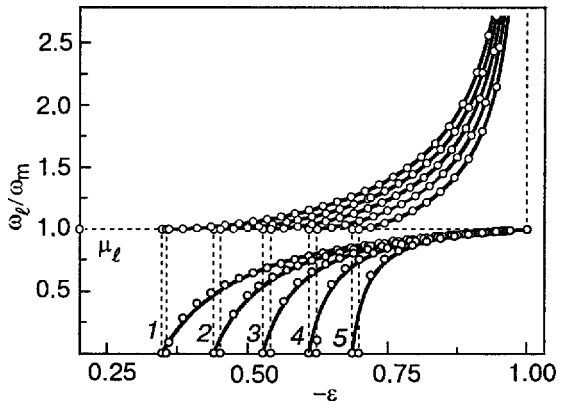

FIG. 9. Plot of the frequencies and intensities of the local modes versus the mass defect for an isolated substitutional impurity in an fcc crystal lattice with a central interaction of nearest neighbors. The interaction of the impurity atom with its neighbors is weaker than the interaction in the host lattice. Curves *1*, *2*, *3*, *4*, and *5* correspond to the values $\Delta\alpha/\alpha=-0.1$, -0.2, -0.3, -0.4, and -0.5. The upper curves are the local mode frequency; the lower curves are the local mode intensity at the impurity atom itself; $n=1$ (solid curves), $n=60$ (points).

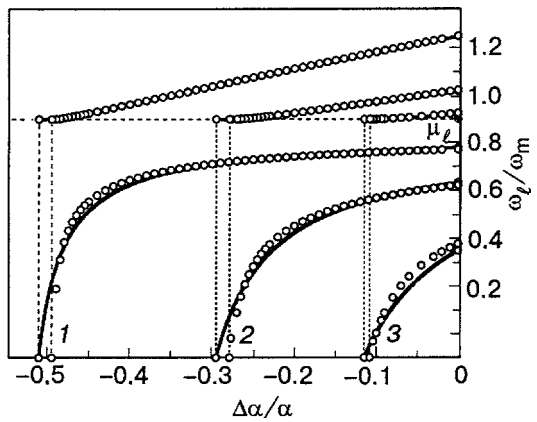

FIG. 10. Change of the frequency and intensity of local modes of a light isolated substitutional impurity in an fcc crystal lattice with a central interaction of nearest neighbors with weakening of the interaction of the impurity atom with its environment; curves *1*, *2*, and *3* correspond to the values of $\Delta m/m$ for impurities of Ar in Xe, Ar in Kr, and Kr in Xe. Upper curves—local mode frequency; lower curves—local mode intensity at the impurity atom itself; $n=1$ (solid curves).

nearest neighbor of the others (in the fcc lattice these are impurity pairs and equilateral triangles and tetrahedra). If the frequency of the local mode is described well by formula (20), then such a local mode is observed in the form a sharp peak even at finite concentrations of the impurity atoms ($c \lesssim 5\%$). For $c \sim 5-10\%$ one should also observe another two peaks, corresponding to in-phase and antiphase displacements of pairs of impurity atoms.[3)] Upon further growth of the concentration these peaks are smeared out, merge together, and form a vibrational impurity band.

The authors are profoundly grateful to A. M. Kosevich, A. S. Kovalev, and E. S. Syrkin, for fruitful discussions and valuable comments.

APPENDIX

In this Appendix we give the values of the threshold mass defects (as arguments of Θ functions) and the dependences of the local frequencies ω_l, intensities μ_0, and damping parameters q on the mass defect for local modes due to various displacements of isolated pairs of light isotopic substitutional impurities which are nearest neighbors, third-nearest neighbors, and fourth-nearest neighbors with each other. These dependences can serve for identification of the various local modes arising at low ($\sim 1-5\%$) concentrations of impurity atoms.

Six mutually orthogonal eigen displacements of a pair of nearest neighbors in the fcc crystal lattice and the mutually orthogonal cyclic subspaces generated by these displacements (by the generating vectors $\vec{h}_0$ transform according to the irreducible representations τ^1-τ^8 of the group O_h (Ref. 34). We present below for each of these subspaces the following information: the index of the corresponding representation, the corresponding generating vector $\vec{h}_0$, the values of the matrix elements a_0 and b_0 of the *ideal* fcc crystal lattice in those subspaces, the dependence of the parameters η and β (18) and of the main parameters of the local mode on the mass defect ε [Eq. (16)]:

$$\tau^1{:}\vec{h}_0 = \frac{1}{2}\left| \begin{matrix} 0, & 0, & 0 \\ \frac{a}{2}, & \frac{a}{2}, & 0 \end{matrix} \right| \begin{matrix} 1 & 1 & 0 \\ -1 & -1 & 0 \end{matrix} \Bigg\rangle;$$

$$a_0 = \frac{5}{8}; \quad \eta(\varepsilon) = \frac{4\varepsilon - 1}{5};$$

$$b_0 = \frac{\sqrt{14}}{16}; \quad \beta(\varepsilon) = \frac{8\varepsilon + 1}{7};$$

$$\begin{cases} \omega_l^2 = \left(\frac{\omega_m}{4}\right)^2 \frac{52|\varepsilon| - 17 + 7\sqrt{26|\varepsilon| - 1}}{(1 - |\varepsilon|)(8|\varepsilon| - 1)}; \\ \mu_0 = \frac{7(1 + 4|\varepsilon|) + (16|\varepsilon| - 9)\sqrt{26|\varepsilon| - 1}}{2(8|\varepsilon| - 1)\sqrt{26|\varepsilon| - 1}} \Theta\left(-\frac{5}{32} - \varepsilon\right); \\ q = \left(2\frac{1 + 4|\varepsilon| - \sqrt{26|\varepsilon| - 1}}{8|\varepsilon| - 1}\right)^2; \end{cases} \tag{A1}$$

$$\tau^3{:}\vec{h}_0 = \frac{1}{2}\left| \begin{matrix} 0, & 0, & 0 \\ \frac{a}{2}, & \frac{a}{2}, & 0 \end{matrix} \right| \begin{matrix} 1 & -1 & 0 \\ -1 & 1 & 0 \end{matrix} \Bigg\rangle;$$

$$a_0 = \frac{1}{2}; \quad \eta(\varepsilon) = \varepsilon;$$

$$b_0 = \frac{\sqrt{14}}{16}; \quad \beta(\varepsilon) = \frac{8\varepsilon + 1}{7};$$

$$\begin{cases} \omega_l^2 = \left(\frac{\omega_m}{4}\right)^2 \frac{4(9|\varepsilon| - 2) + 7\sqrt{2(9|\varepsilon| - 1)}}{(8|\varepsilon| - 1)(1 - |\varepsilon|)}; \\ \mu_0 = \frac{14\sqrt{2}|\varepsilon| + (16|\varepsilon| - 9)\sqrt{9|\varepsilon| - 1}}{2(8|\varepsilon| - 1)\sqrt{9|\varepsilon| - 1}} \Theta\left(-\frac{9}{32} - \varepsilon\right); \\ q = \left(2\frac{4|\varepsilon| - \sqrt{2(9|\varepsilon| - 1)}}{8|\varepsilon| - 1}\right)^2; \end{cases} \tag{A2}$$

$$\tau^4{:}\vec{h}_0 = \frac{1}{\sqrt{2}}\left| \begin{matrix} 0, & 0, & 0 \\ \frac{a}{2}, & \frac{a}{2}, & 0 \end{matrix} \right| \begin{matrix} 0 & 0 & 1 \\ 0 & 0 & 1 \end{matrix} \Bigg\rangle;$$

$$a_0 = \frac{1}{2}; \quad \eta(\varepsilon) = \varepsilon;$$

$$b_0 = \frac{\sqrt{5}}{8}; \quad \beta(\varepsilon) = \frac{4\varepsilon - 1}{5};$$

$$\begin{cases} \omega_l^2 = \left(\frac{\omega_m}{2}\right)^2 \frac{4 + 6|\varepsilon| + 5\sqrt{1 + 3|\varepsilon|}}{2(1 - |\varepsilon|)(1 + 4|\varepsilon|)}; \\ \mu_0 = \frac{10|\varepsilon| + (8|\varepsilon| - 3)\sqrt{1 + 3|\varepsilon|}}{2(1 + 4|\varepsilon|)\sqrt{1 + 3|\varepsilon|}} \Theta\left(-\frac{3}{16} - \varepsilon\right); \\ q = \left(2\frac{2|\varepsilon| - \sqrt{1 + 3|\varepsilon|}}{1 + 4|\varepsilon|}\right)^2; \end{cases} \tag{A3}$$

$$\tau^5{:}\vec{h}_0 = \frac{1}{\sqrt{2}}\left| \begin{matrix} 0, & 0, & 0 \\ \frac{a}{2}, & \frac{a}{2}, & 0 \end{matrix} \right| \begin{matrix} 0 & 0 & 1 \\ 0 & 0 & -1 \end{matrix} \Bigg\rangle;$$

$$a_0 = \frac{1}{2}; \quad \eta(\varepsilon) = \varepsilon;$$

$$b_0 = \frac{\sqrt{3}}{8}; \quad \beta(\varepsilon) = \frac{4\varepsilon + 1}{3};$$

$$\begin{cases} \omega_l^2 = \left(\dfrac{\omega_m}{2}\right)^2 \dfrac{2(5|\varepsilon|-2)+3\sqrt{5|\varepsilon|-1}}{2(1-|\varepsilon|)(4|\varepsilon|-1)}; \\ \mu_0 = \dfrac{6|\varepsilon|+(8|\varepsilon|-5)\sqrt{5|\varepsilon|-1}}{2(4|\varepsilon|-1)\sqrt{5|\varepsilon|-1}}\Theta\left(-\dfrac{5}{16}-\varepsilon\right); \\ q = \left(2\dfrac{2|\varepsilon|-\sqrt{5|\varepsilon|-1}}{4|\varepsilon|-1}\right)^2; \end{cases} \qquad \text{(A4)}$$

$$\tau^6{:}\vec{h}_0 = \frac{1}{2}\left| \begin{matrix} 0, & 0, & 0 \\ \dfrac{a}{2}, & \dfrac{a}{2}, & 0 \end{matrix} \right| \begin{matrix} 1 & -1 & 0 \\ 1 & -1 & 0 \end{matrix} \Bigg\rangle;$$

$$a_0 = \frac{1}{2}; \quad \eta(\varepsilon) = \varepsilon;$$

$$b_0 = \frac{3\sqrt{2}}{16}; \quad \beta(\varepsilon) = \frac{8\varepsilon-1}{9};$$

$$\begin{cases} \omega_l^2 = \left(\dfrac{\omega_m}{4}\right)^2 \dfrac{4(1+7|\varepsilon|)+9\sqrt{2(1+7|\varepsilon|)}}{(1-|\varepsilon|)(1+8|\varepsilon|)}; \\ \mu_0 = \dfrac{36|\varepsilon|+(16|\varepsilon|-7)\sqrt{2(1+7|\varepsilon|)}}{2(1+8|\varepsilon|)\sqrt{2(1+7|\varepsilon|)}}\Theta\left(-\dfrac{7}{32}-\varepsilon\right); \ O_h \\ q = \left(2\dfrac{4|\varepsilon|-\sqrt{2(1+7|\varepsilon|)}}{1+8|\varepsilon|}\right)^2; \end{cases} \qquad \text{(A5)}$$

$$\tau^8{:}h_0 = \frac{1}{2}\left| \begin{matrix} 0, & 0, & 0 \\ \dfrac{a}{2}, & \dfrac{a}{2}, & 0 \end{matrix} \right| \begin{matrix} 1 & 1 & 0 \\ 1 & 1 & 0 \end{matrix} \Bigg\rangle;$$

$$a_0 = \frac{3}{8}; \quad \eta(\varepsilon) = \frac{4\varepsilon+1}{3};$$

$$b_0 = \frac{\sqrt{10}}{16}; \quad \beta(\varepsilon) = \frac{8\varepsilon+3}{5};$$

$$\begin{cases} \omega_l^2 = \left(\dfrac{\omega_m}{4}\right)^2 \dfrac{28|\varepsilon|+13+5\sqrt{14|\varepsilon|-5}}{(1-|\varepsilon|)(8|\varepsilon|-3)}; \\ \mu_0 = \dfrac{5(4|\varepsilon|-1)+(16|\varepsilon|-11)\sqrt{14|\varepsilon|-5}}{2(8|\varepsilon|-3)\sqrt{14|\varepsilon|-5}}\Theta\left(-\dfrac{15}{32}-\varepsilon\right); \\ q = \left(2\dfrac{(1-4|\varepsilon|+\sqrt{14|\varepsilon|-5})}{8|\varepsilon|-3}\right)^2. \end{cases} \qquad \text{(A6)}$$

For the case of the fcc crystal lattice with a central interaction between nearest neighbors in the subspace generated by displacement of each atom, the next-nearest neighbors do not contribute to the matrix elements a_0 and b_0 nor to the two first moments of the spectral density. Therefore, if two isotopic impurities are next-nearest neighbors of each other, then the characteristics of the local modes for each pair of impurities will be described by expressions (32)–(34), even though there is an intersection of the sets of atoms with which each of them interacts.

Below we present the generating vectors and the dependence on ε of the main characteristics of the local modes for different mutually orthogonal displacements of the isolated pairs of isotopic impurities that are third- and fourth-nearest neighbors of each other:

$$\vec{h}_0 = \frac{1}{2\sqrt{3}}\left| \begin{matrix} 0, & 0, & 0 \\ \dfrac{a}{2}, & \dfrac{a}{2}, & a \end{matrix} \right| \begin{matrix} 1 & 1 & 2 \\ 1 & 1 & 2 \end{matrix} \Bigg\rangle;$$

$$a_0 = \frac{1}{2}; \quad \eta(\varepsilon) = \varepsilon;$$

$$b_0 = \frac{\sqrt{19}}{16}; \quad \beta(\varepsilon) = \frac{16\varepsilon-3}{19};$$

$$\begin{cases} \omega_l^2 = \left(\dfrac{\omega_m}{4}\right)^2 \dfrac{4(13|\varepsilon|+6)+19\sqrt{13|\varepsilon|+3}}{(1-|\varepsilon|)(16|\varepsilon|+3)}; \\ \mu_0 = \dfrac{76|\varepsilon|+(32|\varepsilon|-13)\sqrt{13|\varepsilon|+3}}{2(16|\varepsilon|+3)\sqrt{13|\varepsilon|+3}}\Theta\left(-\dfrac{13}{64}-\varepsilon\right); \\ q = \left(4\dfrac{4|\varepsilon|-\sqrt{13|\varepsilon|+3}}{16|\varepsilon|+3}\right)^2; \end{cases} \qquad \text{(A7)}$$

$$\vec{h}_0 = \frac{1}{2\sqrt{3}}\left| \begin{matrix} 0, & 0, & a \\ \dfrac{a}{2}, & \dfrac{a}{2}, & a \end{matrix} \right| \begin{matrix} 1 & 1 & 2 \\ -1 & -1 & -2 \end{matrix} \Bigg\rangle;$$

$$a_0 = \frac{1}{2}; \quad \eta(\varepsilon) = \varepsilon;$$

$$b_0 = \frac{\sqrt{13}}{16}; \quad \beta(\varepsilon) = \frac{16\varepsilon+3}{13};$$

$$\begin{cases} \omega_l^2 = \left(\dfrac{\omega_m}{4}\right)^2 \dfrac{4(19|\varepsilon|-6)+13\sqrt{19|\varepsilon|-3}}{(1-|\varepsilon|)(16|\varepsilon|-3)}; \\ \mu_0 = \dfrac{52|\varepsilon|+(32|\varepsilon|-19)\sqrt{19|\varepsilon|-3}}{2(16|\varepsilon|-3)\sqrt{19|\varepsilon|-3}}\Theta\left(-\dfrac{19}{64}-\varepsilon\right); \\ q = \left(4\dfrac{4|\varepsilon|-\sqrt{19|\varepsilon|-3}}{16|\varepsilon|-3}\right)^2; \end{cases} \qquad \text{(A8)}$$

$$\vec{h}_0 = \frac{1}{2\sqrt{3}}\left| \begin{matrix} 0, & 0, & 0 \\ \dfrac{a}{2}, & \dfrac{a}{2}, & a \end{matrix} \right| \begin{matrix} 1 & -1 & 0 \\ 1 & -1 & 0 \end{matrix} \Bigg\rangle;$$

$$a_0 = \frac{1}{2}; \quad \eta(\varepsilon) = \varepsilon;$$

$$b_0 = \frac{\sqrt{17}}{16}; \quad \beta(\varepsilon) = \frac{16\varepsilon-1}{17};$$

$$\begin{cases} \omega_l^2 = \left(\dfrac{\omega_m}{4}\right)^2 \dfrac{4(15|\varepsilon|+2)+17\sqrt{15|\varepsilon|+1}}{(1-|\varepsilon|)(16|\varepsilon|+1)}; \\ \mu_0 = \dfrac{68|\varepsilon|+(32|\varepsilon|-15)\sqrt{15|\varepsilon|+1}}{2(16|\varepsilon|+1)\sqrt{15|\varepsilon|+1}}\Theta\left(-\dfrac{15}{64}-\varepsilon\right); \\ q = \left(4\dfrac{4|\varepsilon|-\sqrt{15|\varepsilon|+1}}{16|\varepsilon|+1}\right)^2; \end{cases} \tag{A9}$$

$$\vec{h}_0 = \frac{1}{2\sqrt{3}}\left| \begin{matrix} 0, & 0, & a \\ \dfrac{a}{2}, & \dfrac{a}{2}, & a \end{matrix} \right| \begin{matrix} 1 & -1 & 0 \\ -1 & 1 & 0 \end{matrix} \Bigg\rangle;$$

$$a_0 = \frac{1}{2}; \quad \eta(\varepsilon) = \varepsilon;$$

$$b_0 = \frac{\sqrt{15}}{16}; \quad \beta(\varepsilon) = \frac{16\varepsilon+1}{15};$$

$$\begin{cases} \omega_l^2 = \left(\dfrac{\omega_m}{4}\right)^2 \dfrac{4(17|\varepsilon|-2)+15\sqrt{17|\varepsilon|-1}}{(1-|\varepsilon|)(16|\varepsilon|-1)}; \\ \mu_0 = \dfrac{60|\varepsilon|+(32|\varepsilon|-17)\sqrt{17|\varepsilon|-1}}{2(16|\varepsilon|-1)\sqrt{17|\varepsilon|-1}}\Theta\left(-\dfrac{17}{64}-\varepsilon\right); \\ q = \left(4\dfrac{4|\varepsilon|-\sqrt{17|\varepsilon|-1}}{16|\varepsilon|-1}\right)^2; \end{cases} \tag{A10}$$

$$\vec{h}_0 = \frac{1}{2\sqrt{3}}\left| \begin{matrix} 0, & 0, & 0 \\ \dfrac{a}{2}, & \dfrac{a}{2}, & a \end{matrix} \right| \begin{matrix} 1 & 1 & -1 \\ \pm 1 & \pm 1 & \mp 1 \end{matrix} \Bigg\rangle;$$

$$a_0 = \frac{1}{2}; \quad \eta(\varepsilon) = \beta(\varepsilon) = \varepsilon; \quad b_0 = \frac{1}{4}; \tag{A11}$$

the quantities ω_l^2, μ_0, and q are determined by expressions (32)–(34), respectively.

$$\vec{h}_0 = \frac{1}{2}\left| \begin{matrix} 0, & 0, & 0 \\ a, & a, & 0 \end{matrix} \right| \begin{matrix} 1 & 1 & 0 \\ 1 & 1 & 0 \end{matrix} \Bigg\rangle;$$

$$a_0 = \frac{1}{2}; \quad \eta(\varepsilon) = \varepsilon;$$

$$b_0 = \frac{\sqrt{3}}{8}; \quad \beta(\varepsilon) = \frac{4\varepsilon-1}{5}; \tag{A12}$$

the quantities ω_l^2, μ_0, and q are determined by expressions (A3)

$$h_0 = \frac{1}{2}\left| \begin{matrix} 0, & 0, & 0 \\ a, & a, & 0 \end{matrix} \right| \begin{matrix} 1 & 1 & 0 \\ -1 & -1 & 0 \end{matrix} \Bigg\rangle;$$

$$a_0 = \frac{1}{2}; \quad \eta(\varepsilon) = \varepsilon;$$

$$b_0 = \frac{\sqrt{5}}{8}; \quad \beta(\varepsilon) = \frac{4\varepsilon+1}{5}; \tag{A13}$$

the quantities ω_l^2, μ_0, and q are determined by expressed (A4).

In all cases for $\varepsilon = \varepsilon^*$ the values $\omega_l = \omega_m$, $\mu_0 = 0$, and $q = 1$, while for $\varepsilon \to -1$ one has $\omega_{l\to\infty}$, $\mu_0 \to 1$, and $q \to 0$.

[a]E-mail: kotlyar@ilt.kharkov.ua

[1]The vectors of space H will be denoted by arrows over the corresponding symbols, as distinct from the usual three-dimensional vectors which are denoted by boldface symbols.

[2]Both of these metals have an fcc crystal lattice, with lattice constants of ≈4.04 Å for Al and ≈4.08 Å for Ag.[19]

[3]In the case of insufficient power of the defect the local frequency corresponding to the in-phase displacements may remain inside the continuum band.

[1] I. M. Lifshits, Zh. Éksp. Teor. Fiz. **12**, 156 (1942).
[2] I. M. Lifshits, Dokl. Akad. Nauk SSSR **48**, 83 (1945).
[3] I. M. Lifshits, Zh. Éksp. Teor. Fiz. **17**, 1076 (1948).
[4] I. M. Lifshitz, Nuovo Cim. Suppl. **3**, 716 (1956) [Russ. trans. in I. M. Lifshits, *Collected Works*, Vol. 1, Nauka, Moscow (1987), p. 106].
[5] I. M. Lifshitz and A. M. Kosevich, Rep. Prog. Phys. **29**, 217 (1966) [Russ. trans. in I. M. Lifshits, *Collected Works*, Vol. 1, Nauka, Moscow (1987), p. 142].
[6] I. M. Lifshits, Usp. Mat. Nauk **7**, 171 (1952).
[7] A. M. Kosevich, *Theory of the Crystal Lattice (Physical Mechanics of Crystals)* [in Russian], Vishcha Shkola, Kharkov (1988).
[8] A. M. Kossevich, *The Crystal Lattice (Phonons, Solitons, Dislocations)*, WILEY-VCH Verlag Berlin GmBH, Berlin (1999).
[9] A. A. Maradudin, E. W. Montroll, and G. H. Weiss, in *Solid State Physics*, Suppl. 3, Academic Press, New York (1963) [Russ. trans., *Dynamical Theory of the Crystal Lattice in the Harmonic Approximation*, Mir, Moscow (1965)].
[10] A. A. Maradudin, Solid State Phys. **18**, 273 (1966); **19**, 1 (1966) [Russ. trans., *Defects and the Vibrational Spectrum of Crystals*, Mir, Moscow (1968)].
[11] H. Bettger, *Principles of the Theory of Lattice Dynamics*, Akademie-Verlag, Berlin (1983), Mir, Moscow (1986).
[12] Yu. G. Naĭdyuk, N. A. Chernoplekov, Yu. L. Shitikov, O. I. Shklyarevskiĭ, and I. K. Yanson, Zh. Éksp. Teor. Fiz. **83**, 1177 (1982) [Sov. Phys. JETP **56**, 671 (1982)].
[13] Yu. G. Naĭdyuk, I. K. Yanson, A. A. Lysykh, and Yu. L. Shitikov, Fiz. Tverd. Tela (Leningrad) **26**, 2734 (1984) [Sov. Phys. Solid State **26**, 1656 (1984)].
[14] L. A. Falkovsky, JETP Lett. **71**, 155 (2000).
[15] L. A. Falkovsky, Zh. Éksp. Teor. Fiz. **117**, 735 (2000) [JETP **90**, 639 (2000)].
[16] M. A. Ivanov and Yu. V. Skripnik, Fiz. Tverd. Tela (St. Petersburg) **34**, 641 (1992) [Phys. Solid State **34**, 342 (1992)].
[17] M. A. Ivanov and Yu. V. Skripnik, Fiz. Tverd. Tela (St. Petersburg) **36**, 94 (1994) [Phys. Solid State **36**, 51 (1994)].
[18] O. Braun and Yu. S. Kivshar, Phys. Rep. **306** (1998).
[19] G. Leibfried and N. Breuer, *Point Defects in Metals I*, Springer-Verlag, Berlin (1978), Mir, Moscow (1981).
[20] V. I. Peresada, Doctoral Dissertation, Kharkov (1972).
[21] V. I. Peresada, *Condensed Matter Physics* [in Russian], FTINT AN UkrSSR, Kharkov (1968), p. 172.
[22] V. I. Peresada, V. N. Afanas'ev, and V. S. Borovikov, Fiz. Nizk. Temp. **1**, 461 (1975) [Sov. J. Low Temp. Phys. **1**, 227 (1975)].
[23] R. Haydock, in *Solid State Physics*, Vol. 35, edited by H. Ehrenreich *et al.*, Academic Press, New York (1980), p. 129.
[24] I. A. Gospodarev, A. V. Grishaev, E. S. Syrkin, and S. B. Feodos'ev, Fiz. Tverd. Tela (St. Petersburg) **42**, 2153 (2000) [Phys. Solid State **42**, 2217 (2000)].
[25] M. A. Mamaluĭ, E. S. Syrkin, and S. B. Feodos'ev, Fiz. Tverd. Tela (St. Petersburg) **38**, 3683 (1996) [Phys. Solid State **38**, 2006 (1996)].
[26] M. A. Mamalui, E. S. Syrkin, and S. B. Feodosyev, Fiz. Nizk. Temp. **24**, 8, 586 (1998) [Low Temp. Phys. **24**, 583 (1998)].
[27] M. A. Mamalui, E. S. Syrkin, and S. B. Feodosev, Fiz. Nizk. Temp. **25**,

586 (1999) [Low Temp. Phys. **25**, 732 (1999)].
[28]G. Szegö, *Orthogonal Polynomials*, American Mathematical Society, New York (1959), Gos. Izd-vo Fiz.-Mat. Lit. Moscow (1962).
[29]N. I. Akhiezer, *The Classical Moment Problem and Some Related Questions in Analysis*, Oliver and Boyd, Edinburgh (1965), Gos. Izd-vo Fiz.-Mat. Lit. Moscow (1961).
[30]V. I. Peresada and V. P. Tolstoluzhskiĭ, "On the influence of impurity atoms on the thermodynamic properties of the face centered cubic lattice" [in Russian], FTINT AN UkrSSR Preprint, B. Verkin Institute for Low Temperature Physics and Engineering, National Academy of Sciences of Ukraine, Kharkov (1970).
[31]V. I. Peresada and V. P. Tolstoluzhskiĭ, Fiz. Nizk. Temp. **3**, 788 (1977) [Sov. J. Low Temp. Phys. **3**, 383 (1977)].
[32]V. N. Afanas'ev, in *Condensed Matter Physics* [in Russian], FTINT AN UkrSSR, Kharkov (1970), p. 10.
[33]G. G. Sergeeva, Zh. Éksp. Teor. Fiz. **48**, 158 (1965) [Sov. Phys. JETP **21**, 108 (1965)].
[34]O. V. Kovalev, *Irreducible Representations of the Space Groups*, Gordon and Breach, New York (1965), Ukrainian Academy of Sciences Press, Kiev (1961).
[35]A. F. Prikhot'ko, V. G. Manzheliĭ, I. Ya. Fugol', Yu. B. Gaĭdideĭ, I. N. Krupskiĭ, V. M. Loktev, E. V. Savchenko, V. A. Slyusarev, M. A. Strzhemechnyĭ, Yu. A. Freĭman, and L. I. Shanskiĭ, *Cryocrystals*, Naukova Dumka, Kiev (1983).
[36]S. B. Feodosyev, I. A. Gospodarev, V. I. Grishaev, and E. S. Syrkin, Fiz. Nizk. Temp. **29**, 710 (2003) [Low Temp. Phys. **29**, 530 (2003)].
[37]S. B. Feodosyev, I. A. Gospodarev, M. A. Mamalui, and E. S. Syrkin, J. Low Temp. Phys. **111**, 441 (1998).

Translated by Steve Torstveit